

Polarization-adjusted Convolutional (PAC) Codes: Fano Decoding vs List Decoding

Mohammad Rowshan, *Student Member, IEEE*, Andreas Burg, *Member, IEEE*,
Emanuele Viterbo, *Fellow, IEEE*

In the Shannon lecture at the 2019 International Symposium on Information Theory (ISIT), Arikan proposed to employ a one-to-one convolutional transform as a pre-coding step before polar transform. The resulting codes of this concatenation are called *polarization-adjusted convolutional (PAC) codes*. In this scheme, a pair of polar mapper and demapper as pre- and post-processing devices are deployed around a memoryless channel, which provides polarized information to an outer decoder leading to improved error correction performance of outer code. In this paper, the implementations of list decoding and Fano decoding for PAC codes are first investigated. Then, in order to reduce the complexity of sequential decoding of PAC/polar codes, we propose (i) an adaptive heuristic metric, (ii) tree search constraints for backtracking to avoid exploration of unlikely sub-paths, and (iii) tree search strategies consistent with the pattern of error occurrence in polar codes. These contribute to reducing the average decoding time complexity up to 85%, with only a relatively small degradation in error correction performance. Additionally, as an important ingredient in Fano decoding of PAC/polar codes, an efficient computation method for the intermediate LLRs and partial sums is provided. This method is necessary for backtracking and avoids storing the intermediate information or restarting the decoding process.

Index Terms—Polarization-adjusted convolutional codes, polar codes, convolutional codes, list decoding, sequential decoding, Fano algorithm, tree search, path metric.

I. INTRODUCTION

Polar codes proposed by Arikan in [1] are the first class of channel codes with explicit construction that was proven to achieve the symmetric (Shannon) capacity of a binary-input discrete memoryless channel (BI-DMC) using a low-complexity successive cancellation (SC) decoder.

Polar codes are founded on the polarization effect resulting from channel synthesizing in a particular fashion. The idea of building synthetic channels was originated from the concatenated schemes [2] employed in the sequential decoding of convolutional codes by Massey [3] and Pinsker [4], in order to boost the cutoff rate. The cutoff rate is said to be "boosted" when the sum of the cutoff rates of the synthesized channels is greater than the sum of the cutoff rates of the raw channels. The key idea in boosting the cutoff rate is to build a

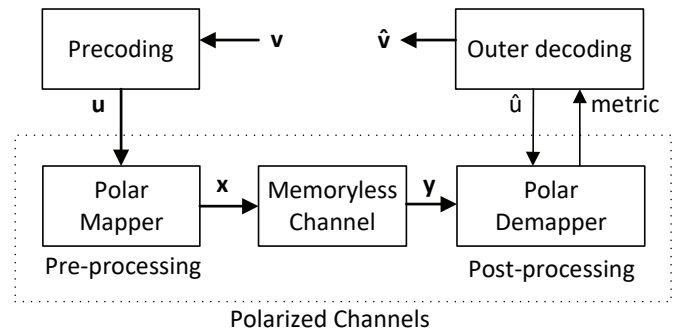


Figure 1. Code Concatenation

vector channel where the independent copies of raw channels are transformed into multiple correlated channels. In Pinsker's scheme, the inner block code (with length N) is suggested to be chosen at random. This requires a maximum likelihood (ML) decoding with prohibitive complexity. Polar codes allow using a more practical decoder with the complexity of $O(N \log N)$. Unlike Pinsker's scheme, where the outer convolutional transforms are identical, in multi-level coding and multi-stage decoding (MLC/MSD)¹, N convolutional codes at different rates $\{R_i\}$ are used which consequently require a chain of N outer convolutional decoders.

On the other hand, polar coding was originally designed as a low-complexity recursive channel combining and splitting operation, where the polarization effect constrains the rates R_i to either 0 or 1. They turned out to be so effective that no outer code was employed to achieve the original aim of boosting the cutoff rate to channel capacity.

Nevertheless, the error correction performance of finite-length polar codes under successive cancellation (SC) decoding is not competitive, due to the existence of partially polarized channels. To address this issue, the successive cancellation list (SCL) decoding was proposed in [6]. This yields an error correction performance comparable to maximum-likelihood (ML) decoding. Also, it was observed that further improvement could be obtained by concatenating cyclic redundancy check (CRC) bits to polar codes.

Recently in [7], Arikan proposed a concatenation of convolutional transform with the polarization transform [1], inspired on the aforementioned schemes in which the message is first encoded using a convolutional transform and then transmitted over polarized synthetic channels as shown in Fig. 1. These

¹Originally proposed in [5] as an efficient coded-modulation technique.

M. Rowshan and E. Viterbo are with the Department of Electrical and Computer Systems Engineering (ECSE), Monash University, Melbourne, VIC3800, Australia. E-mail: {mohammad.rowshan, emanuele.viterbo}@monash.edu. These authors' work was supported by the Australian Research Council under Discovery Project ARC DP160100528.

Andreas Burg is with the Telecommunications Circuits Laboratory (TCL), Swiss Federal Institute of Technology (EPFL), Lausanne 1015, Switzerland E-mail: andreas.burg@epfl.ch.

codes are called “polarization-adjusted convolutional (PAC) codes”. The results show that the block error rate performance of this scheme can reach the finite-length capacity bound [8] a.k.a. dispersion bound.

This paper is concerned with the implementation of Fano and list decoders, and compares the numerical results with polar codes in terms of error correction performance and complexity. The contributions of this work are given below.

- The Fano decoding algorithm requires backtracking during the binary tree search, hence intermediate log-likelihood ratios (LLRs) and partial sums need to be updated. This should be performed without restarting the decoding operation or storing more than $2N - 1$ intermediate LLRs and partial sums as in conventional SC decoding, [10]. In this work, an efficient approach to compute the intermediate LLRs and partial sums, is proposed.
- The Fano metric is modified in order to improve the comparability of (unexplored) variable-length paths with the current path. Furthermore, an adaptive bias is proposed to adjust the bias-term in the metric relative to the impact of the channel noise on the metric. This adaptive metric can reduce significantly the number of visited nodes.
- A tree search strategy is proposed in which the number of diverging paths from the current best path is limited. This is equivalent to constraining the search to the paths in which there are a limited number of flipped bits. Further, this strategy is applied only to the set of bit indices where over 99% of the errors occur. This set, which is called *critical set*, can reduce the time complexity by visiting less nodes at the cost of negligible degradation.
- A combination of *top-down* search and *bottom-up* search strategies for the tree search algorithm are proposed to adapt the Fano algorithm to the pattern of error occurrence in polar codes, which helps in finding the correct path faster.
- A performance comparison (relative to dispersion bound) of Fano decoding with list decoding for PAC codes, with or without CRC concatenation, for different list sizes and code-lengths, is provided by simulation.

Paper Outline: Section II introduces the notations for polar codes and convolutional codes and describes their decoding algorithms. Section III illustrates polarization-adjusted convolutional transform, and describes the decoding algorithms. In Section IV, first, an efficient method for calculating the intermediate LLRs and partial sums required through backtracking in Fano decoding is proposed. Then, a heuristic path metric for Fano decoding is introduced. In Section V, strategies are described to improve Fano decoding including adaptive path metric, tree search strategies and search constraints. In Section VI, the distance properties of PAC codes and polar codes are compared and the implementation results are shown. Finally Section VII provides some concluding remarks.

II. PRELIMINARIES

Polarization-adjusted codes are special concatenation scheme based on polar transform as inner coding scheme

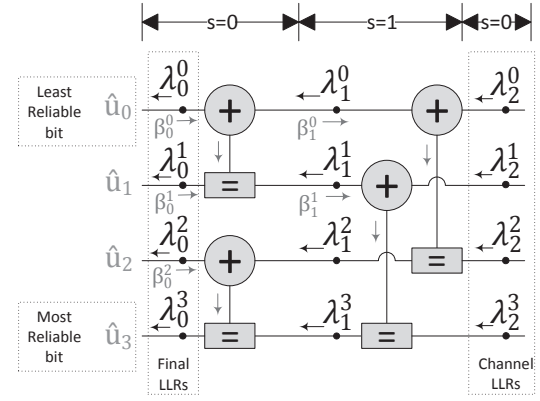


Figure 2. Successive cancellation factor graph for $N = 4$

and convolution transform as outer coding scheme. Hence, let us first introduce polar coding and convolutional coding as standalone coding schemes.

A. Polar Codes

A polar code of length $N = 2^n$ with K information bits is denoted by $P(N, K, \mathcal{A})$, where \mathcal{A} is the data index set. The information bits d of length K is embedded in the vector u such that $u_{\mathcal{A}} = d$, and $u_{\mathcal{A}^c} = 0$ which are called frozen bits. The set \mathcal{A} constitutes of indices of reliable bit-channels based on the polarization phenomenon.

A polar code is obtained from $x_0^{N-1} = u_0^{N-1} P_n$, where the *polar transform* P_n is defined as the n -th Kronecker power of $P \triangleq \begin{bmatrix} 1 & 0 \\ 1 & 1 \end{bmatrix}$, i.e $P_n = P^{\otimes n}$. Let $y_0^{N-1} = (y_0, y_1, \dots, y_{N-1})$ denote the output vector of a noisy channel.

The standard decoding method for polar codes is successive cancellation (SC) decoding in which the non-frozen bits are estimated successively based on the evolved log-likelihood ratio (LLR), denoted by λ_s^i , via a one-time-pass through the factor graph in Fig. 2. Successive hard decisions make the SC solution sub-optimal. When decoding the i -th bit, if $i \notin \mathcal{A}$, $\hat{u}_i = 0$, as u_i is a frozen bit. Otherwise, bit u_i is decided by a local maximum likelihood (ML) rule $h(\lambda_0^i)$ in (1), which depends on the estimation of previous bits, i.e., $\hat{u}_0, \dots, \hat{u}_{i-1}$.

$$\hat{u}_i = h(\lambda_0^i) = \begin{cases} 0 & \lambda_0^i = \ln \frac{P(Y, \hat{u}_0^{i-1} | \hat{u}_i=0)}{P(Y, \hat{u}_0^{i-1} | \hat{u}_i=1)} > 0, \\ 1 & \text{otherwise} \end{cases} \quad (1)$$

To resolve the problem of potentially erroneous decisions in the SC decoding, we can introduce the notion of a binary decision tree. In this tree, each branch on level i corresponds to a decision for $u_i = 1$ or $u_i = 0$ and a path from the root to a leaf corresponds to a decoded codeword. SC decoding explores only a single path of this tree. Let us denote the *SC path* as the path in the tree obtained by following the branches with the larger likelihood (these branches are called *good branches* and the alternative ones are called *bad branches* throughout this paper) at every decoding step. By exploring multiple or all paths, erroneous preliminary decisions can be corrected to potentially reach ML performance.

Since exhaustive exploration of the tree is prohibitively complex, SC list (SCL) decoding [6] performs a constrained

breadth-first search (proceeding from the root to the leaves) which tracks only up to L parallel paths, that are deemed to be the most reliable ones based on the local decisions.

Let $\hat{u}_i[l]$ denote the estimate of u_i in the l -th path, where $l \in \{1, 2, \dots, L\}$. In [9], unlike [6], a path metric (PM) based on LLRs magnitudes is used to measure the reliability of each path to make local decisions on which path to keep and which to drop. The PM at $\hat{u}_i[l]$ is approximated by

$$PM_l^{(i)} = \begin{cases} PM_l^{(i-1)} + |\lambda_0^i[l]| & \text{if } \hat{u}_i[l] \neq \frac{1}{2}(1 - \text{sgn}(\lambda_0^i[l])) \\ PM_l^{(i-1)} & \text{otherwise} \end{cases} \quad (2)$$

where $PM_l^{(-1)} = 0$.

As (2) shows, the path of the less likely bit value is penalized by $|\lambda_0^i[l]|$ of that bit. The L paths with the smallest path metrics are chosen from $2L$ paths at each step (level of the tree) and are stored in ascending order from $PM_1^{(i)}$ to $PM_L^{(i)}$. At the leaf (N -th step), the path with the smallest path metric $PM_1^{(N)}$ is selected as the estimated codeword.

Additionally, to compensate for the known poor distance properties of polar codes, an r -bit CRC is appended to the message as an outer code to assist the decoder in error detection and finding the correct path among the L paths in the list. However, this concatenation increases the polar code rate to $(K+r)/N$ causing a small performance degradation in the low SNR regime.

B. Convolutional Codes

Convolutional codes (CC) [15] are a class of linear codes described by a tuple (n_0, k, m) , where k is the number of information bits shifted into the encoder at each time slot (usually $k = 1$), n_0 is the number of corresponding outputted coded bits, and m is the number of previous input bits stored in a shift-register. The shift-register based encoder is equivalent to a sliding window over the information bit sequence to calculate $n_0 > 1$ coded bits by combining (using binary addition) various subsets of the bits in the window (see Fig. 3). The code rate is given by k/n_0 . The size of the window $m+1$, in bits, is called the *constraint length* of the code and is shifted by k bits every time. The constraint length determines the number of previous input bits plus the current bit that influence each coded bit. A larger constraint length generally provides greater resilience to bit errors.

The relation between the input information bits d_{i-m}^i and one of the n_0 output bits x_i , at time i , is obtained as a binary convolution $x_i = \sum_{j=0}^m g_j d_{i-j}$, where $g_i \in \{0, 1\}$. By representing bit sequences as polynomials in the delay variable D representing a clock cycle in the encoder, an output sequence $x(D)$ is obtained as $g(D)d(D)$, where $g(D) = \sum_{j=0}^m g_j D^j$ is the *generator polynomial*. Different generator polynomials are used for each of the n_0 outputs.

Equivalently, this can be represented in matrix form where the rows of an upper-triangular *generator matrix* G are formed by shifting the vector $\mathbf{g} = (g_0, \dots, g_m)$. The number of rows equals the block-length. Given the generator matrix \mathbf{G} , we can encode the message block \mathbf{v} as $\mathbf{u} = \mathbf{v}\mathbf{G}$. In the case

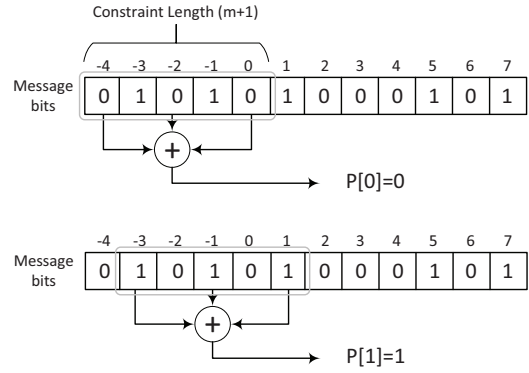


Figure 3. Sliding parity bit calculation

where $n_0 = k = 1$ we have unit rate code which results in a one-to-one linear transformation of the input sequence.

Convolutional codes are decoded using the trellis-based Viterbi algorithm and the tree search sequential decoding algorithms. The Viterbi algorithm is a maximum likelihood decoding method that examines the total encoder's state space at each step. Consequently, the space complexity (storage requirement) of the Viterbi algorithm grows exponentially with the constraint length $m+1$ of the encoder. However, by making a decision about the correct path after decoding every short-length sequence and truncating the path memory for the rest of the paths, the space complexity is constrained at the cost of insignificant degradation in error rate performance [17].

On the other hand, the complexity of sequential decoding is essentially independent of the encoder's memory, since only one encoder state is examined at each step. The fundamental idea behind sequential decoding is to explore only the most promising path(s). If a path to a node looks "bad" we can discard all the paths stemming from it without a significant loss in the error correction performance from that of a maximum likelihood decoder [18].

In this work, we focus on Fano decoding which is a memory-efficient type of Sequential decoding algorithm. The *Fano algorithm* is a depth-first tree search, in which the decoder moves from a node to either back to its parent node or to one of its children. The Fano decoder can visit a node only if its Fano path metric μ_F is larger than or equal to a certain value called threshold T . Threshold takes only discrete values $0, \pm\Delta, \pm2\Delta, \dots$

In comparison with the decoding algorithms discussed in Section II-A, the following points about SC and SC list decoding should be noted: The SC decoding makes decisions to choose the node to visit at each step based on the branch metric. Thus, only one path is explored and the rest are discarded. In contrast, in the SC list decoding, the L paths explored on the decoding tree have the same length and the most promising ones are retained at each time step. Thus, no backtracking is performed in SC and SC list decoding. Additionally, the path metric used to measure the likelihood of the paths in the sequential decoding considers the difference in the lengths of partial paths by adding a bias, while in the SC list decoding, the bias term is not required.

The metric used in the Fano sequential decoding of convolutional codes is a probabilistic path metric. We consider

the set $\mathcal{X} = \{a^{(1)}, a^{(2)}, \dots, a^{(M)}\}$ of M partial sequences, representing partially explored paths with different lengths, to be compared. Let $n_{max} = \max\{n_1, n_2, \dots, n_M\}$ denote the length of longest sequence, and \mathbf{r} the received sequence of length n corresponding to a transmitted codeword. Among the sequences in \mathcal{X} , we choose the partial sequence $a^{(\ell)}$ that maximizes the a-posterior probability $P(a^{(\ell)}|\tilde{\mathbf{r}})$ where $\tilde{\mathbf{r}} = (r_0, r_1, \dots, r_{n_{max}-1})$ is the received sub-vector corresponding to the longest sequence. According to Bayes' rule

$$P(a^{(\ell)}|\tilde{\mathbf{r}}) = \frac{P(a^{(\ell)})P(\tilde{\mathbf{r}}|a^{(\ell)})}{P(\tilde{\mathbf{r}})} \quad (3)$$

Assuming the channels are memoryless, we have

$$P(\tilde{\mathbf{r}}|a^{(\ell)}) = \prod_{j=0}^{n_i-1} P(r_j|a_j^{(\ell)}) \prod_{j=n_i}^{n_{max}-1} P(r_j)$$

and $P(a^{(\ell)}) = (2^{-k})^{n_i} = (2^{-nR})^{n_i}$. By simplifying and taking the base-2 logarithm of (3) we have

$$\log P(a^{(\ell)}|\tilde{\mathbf{r}}) = \sum_{j=0}^{n_i-1} \underbrace{\left(\log P(r_j|a_j^{(\ell)}) - \log P(r_j) - R \right)}_{\text{ML-metric}} \quad (4)$$

In the computer science literature, the path metric of algorithm A, a graph traversal and path search algorithm, is written in the general form of [19]

$$f(a^{(\ell)}) = g(a^{(\ell)}) + h(a^{(\ell)}) \quad (5)$$

where the first term measures the actual cost of the i -th partial path as follows,

$$g(a^{(\ell)}) = \sum_{j=0}^{n_i-1} \log P(r_j|a_j^{(\ell)}) \quad (6)$$

and the second term is a heuristic estimate for the remaining cost of completing the path to its leaf with the best metric by following the corresponding (yet unknown) extension of $a^{(\ell)}$. The choice of the heuristic function $h(a^{(\ell)})$, determines the tradeoff between the complexity and the risk of accidentally abandoning a path that leads to the desired optimal solution.

We propose a heuristic to estimate $h(a^{(\ell)})$ for Fano decoding of polar codes and PAC codes in Section V-A.

III. POLARIZATION-ADJUSTED CODES

Polarization-adjusted convolutional codes, denoted by $PAC(N, K, \mathcal{B}, c)$, are based on the outer convolutional transform and inner polar coding. In PAC codes, rate profiling is performed before the convolutional transform, in which the information bits are assigned to the positions in the index set \mathcal{B} and 0 to the rest. The pre-coding stage is a one-to-one convolutional transform and the mapper is the polar transform. One may consider PAC coding as a polar coding scheme in which the inputs to the frozen bit-channels are linear combinations of previous bits obtained by convolutional transforms. In fact, these formerly frozen bits are acting as parity check (PC) bits [27] or dynamic frozen bits [28]. Thus, given that the previous bits have been estimated correctly, the decoder can still determine the value transmitted by the corresponding "bad channels". Note that fully random input (i.e.

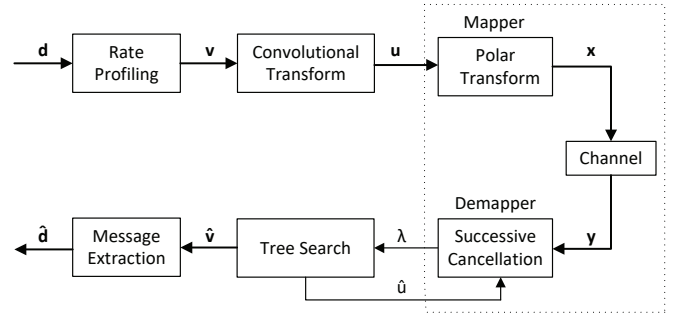


Figure 4. PAC coding scheme

including no frozen bit) to the polar transform increases the output randomness which is expected to improve the distance properties of PAC codes [31]. We examine this hypothesis in Section VI-A. In the following Sections, the encoding and decoding of PAC codes are described in detail.

A. PAC Encoding

The information bits $\mathbf{d} = (d_0, d_1, \dots, d_{k-1})$ are first mapped to a vector $\mathbf{v} = (v_0, v_1, \dots, v_{N-1})$ using a rate-profile. The rate-profile is formed based on the index set \mathcal{B} . This set includes the indices of the positions where the information bits are placed in the input vector to the convolutional transform (CT). The bit values in the remaining positions in \mathbf{v} are set to 0. The constraint $v_{\mathcal{B}^c} = 0$ simply leads to an irregular decoding tree. Note that 1) the outputs of CT for indices in \mathcal{B}^c , which enter the polar transform, are now no longer fixed or known a priori - unlike polar codes. 2) In contrast to conventional convolutional encoders in which usually $R_c < 1$, here, we use a one-to-one transform \mathbf{G} , hence the vectors \mathbf{v} and \mathbf{u} in $\mathbf{u} = \mathbf{v}\mathbf{G}$ have the same dimension.

After the convolutional transform, the vector \mathbf{u} is mapped to \mathbf{x} , as Fig. 4 shows, by employing the polar transform \mathbf{P}_n ; hence, $\mathbf{x} = \mathbf{u}\mathbf{P}_n$. Algorithm 1 summarizes the encoding process.

B. PAC List Decoding

PAC codes as (irregular) tree codes can be decoded using the tree search algorithms discussed in Section II. In the following, we consider the list decoding which trades a fixed complexity for large memory requirements to store a list of paths. In the next section and the rest of the paper, we focus on Fano decoding which has a variable complexity but is much more memory-efficient.

Algorithm 2 illustrates the list decoding approach. In the beginning, there is a single path in the list. When the index of the current bit is in the set \mathcal{B}^c , the decoder knows its value, usually $v_i = 0$ and therefore it is transformed into u_i based on the current memory state $currState$ and the generator polynomial \mathbf{g} in line 6. Then, by obtaining the decision LLR λ_0^i in line 7, the corresponding path metric is calculated as follows: If the sign of the decision LLR is not in line with u_i , the path is penalized and the decoded value u_i is fed back into SC process in line 9 to calculate partial sums. On the other

Algorithm 1: PAC Encoding

input : Information bits \mathbf{d} , N , \mathcal{B} , \mathbf{g}
output: the codeword \mathbf{x}

```
1  $\mathbf{v} \leftarrow \text{rateProfiler}(\mathbf{d}, \mathcal{B}, N)$ 
2  $\mathbf{u} \leftarrow \text{convEncoder}(\mathbf{v}, \mathbf{g})$ 
3  $\mathbf{x} \leftarrow \text{polarEncoder}(\mathbf{u})$ 
4 return  $\mathbf{x}$ ;
5 subroutine  $\text{convEncoder}(\mathbf{v}, \mathbf{g})$ :
6    $\text{cState}[1, \dots, |\mathbf{g}| - 1] \leftarrow [0, \dots, 0]$  // currState
7   for  $i \leftarrow 0$  to  $|\mathbf{v}| - 1$  do
8      $(u_i, \text{cState}) \leftarrow \text{conv1bitEnc}(v_i, \text{cState}, \mathbf{g})$ 
9   return  $\mathbf{u}$ ;
10 subroutine  $\text{conv1bitEnc}(v, \text{currState}, \mathbf{g})$ :
11    $u \leftarrow v \cdot g_0$ 
12   for  $j \leftarrow 1$  to  $|\mathbf{g}|$  do
13     if  $g_j = 1$  then
14        $u \leftarrow u \oplus \text{currState}[j - 1]$ 
15    $\text{nextState} \leftarrow [v_i] + \text{currState}[1, \dots, |\mathbf{g}| - 2]$ 
16   return  $(u, \text{nextState})$ ;
```

hand, if the index of the current bit is in the set \mathcal{B} , there are two options for the value of v_i , 0 and 1, to be considered in line 23. For each option of 0 and 1, the aforementioned process for $i \in \mathcal{B}^c$ including convolutional transform, and calculating path metric is performed and then the two transformed values $u_i = 0$ and 1 are fed back into SC process as mentioned in lines 24-31.

One can notice that the process of list decoding for PAC codes is similar to that for polar codes except for the additional convolutional re-transform at each decoding step for which the next memory state is stored for each path. For medium and long block-lengths, we can also concatenate CRC-bits to the information bits to help in detecting the correct path. To improve the computational complexity and performance of list decoding, the methods proposed in the literature such as in [11], [12] can be applied on PAC list decoding as well.

IV. FANO DECODING OF PAC CODES

List decoding, with its non-backtracking tree search approach, requires the very large list size of $L = 256$ to reach the dispersion bound [8], as it will be shown in Section VI. However, memory-efficient backtracking search algorithms such as the Fano algorithm can approach the dispersion bound at the cost of an extremely high average time complexity.

The Fano algorithm performs forward and backward traversals in the decoding tree: While in the forward traversal, the calculation of the required intermediate LLRs is straightforward and linear, a more sophisticated approach is required for the backward traversal. Suppose we need to move back from the i_{curr} -th bit to the i_{dest} -th bit: First, we need to calculate the decision LLR at bit i_{dest} , $\lambda_0^{i_{\text{dest}}}$, which depends on the intermediate LLRs. As explained in [10], at most $N - 1$ intermediate LLRs need to be stored for decoding bits 0 to $N - 1$, where $N/2^{n-s}$ of which are associated to stage s ($0 \leq s \leq n - 1$). Depending on i_{dest} , none of the intermediate

Algorithm 2: List Decoding of PAC codes

input : the received vector y_1^N , \mathcal{B} , L , \mathbf{g} , $\lambda_n^{0, N-1}$
output: the recovered message bits $\hat{\mathbf{d}}$

```
1  $\mathcal{L} \leftarrow \{1\}$  // a single path in the list
2 for  $i \leftarrow 0$  to  $N - 1$  do
3   if  $i \notin \mathcal{B}$  then
4     for  $l \leftarrow 1$  to  $|\mathcal{L}|$  do
5        $\hat{v}_i[l] \leftarrow v_i$  //  $v_i = 0$  is known
6        $\hat{u}_i[l] \leftarrow \text{conv1bitEnc}(v_i, \text{currState}[l], \mathbf{g})$ 
7        $\lambda_0^i[l] \leftarrow \text{updateLLRs}(l, i, \lambda[l], \beta_l)$ 
8        $PM_l^{(i)} \leftarrow \text{calcPM}(PM_l^{(i-1)}, \lambda_0^i[l], \hat{u}_i[l])$ 
9        $\beta_l \leftarrow \text{updatePartialSums}(\hat{u}_i[l], \beta_l)$ 
10    else
11      for  $l \leftarrow 1$  to  $|\mathcal{L}|$  do
12        if  $|\mathcal{L}| < L$  then
13          foreach  $l \in \mathcal{L}$  do
14             $\text{duplicatePath}(l, i, \mathbf{g})$ 
15          else
16            foreach  $l \in \mathcal{L}$  do
17               $\text{duplicatePath}(l, i, \mathbf{g})$ 
18             $\mathcal{L} \leftarrow \text{prunePaths}(\mathcal{L})$ 
19   $\hat{\mathbf{d}} \leftarrow \text{extractData}(\hat{v}_1^N[0])$ 
20  return  $\hat{\mathbf{d}}$ ;
21 subroutine  $\text{duplicatePath}(l, i, \mathbf{g})$ :
22    $\mathcal{L} \leftarrow \mathcal{L} \cup \{l'\}$  //  $l'$  is a copy of  $l$ 
23    $(\hat{v}_i[l], \hat{v}_i[l']) \leftarrow (0, 1)$ 
24    $\hat{u}_i[l] \leftarrow \text{conv1bitEnc}(\hat{v}_i[l], \text{currState}[l], \mathbf{g})$ 
25    $\hat{u}_i[l'] \leftarrow \text{conv1bitEnc}(\hat{v}_i[l'], \text{currState}[l'], \mathbf{g})$ 
26    $\lambda_0^i[l] \leftarrow \text{updateLLRs}(l, i, \lambda[l], \beta_l)$ 
27    $\lambda_0^i[l'] \leftarrow \text{updateLLRs}(l', i, \lambda[l'], \beta_{l'})$ 
28    $PM_l^{(i)} \leftarrow \text{calcPM}(PM_l^{(i-1)}, \lambda_0^i[l], \hat{u}_i[l])$ 
29    $PM_{l'}^{(i)} \leftarrow \text{calcPM}(PM_{l'}^{(i-1)}, \lambda_0^i[l'], \hat{u}_i[l'])$ 
30    $\beta_l \leftarrow \text{updatePartialSums}(\hat{u}_i[l], \beta_l)$ 
31    $\beta_{l'} \leftarrow \text{updatePartialSums}(\hat{u}_i[l'], \beta_{l'})$ 
32 subroutine  $\text{calcPM}(PM, \lambda_0, \hat{u})$ :
33   if  $\hat{u} = \frac{1}{2}(1 - \text{sgn}(\lambda_0))$  then
34      $PM = PM$ 
35   else
36      $PM = PM + |\lambda_0|$ 
37   return  $PM$ ;
```

LLRs (when moving from bit $2i + 1$ to bit $2i$) or in extreme cases all of $N - 1$ elements should be updated. Hence, updating the intermediate LLRs (partially or fully) might be necessary for backtracking.

In general, up to $\log_2 N$ stages should be activated to calculate the decision LLR at bit i_{dest} , $\lambda_0^{i_{\text{dest}}}$. The first stage to be activated (from right to left in Fig. 2) is determined by *find first set* (ffs) operation, here, *set* means 1, on the binary representation of bit index x , i.e., $\text{bin}(x) = x_{n-1} \dots x_1 x_0$. The modified version of ffs is defined below [10]. Note that we assume the decoding is performed in the natural order, not

bit-reversal.

$$\text{ffs}^*(x_{n-1}\dots x_1x_0) = \begin{cases} \min(j) : x_j = 1 & x > 0, \\ n-1 & x = 0 \end{cases} \quad (7)$$

When i_{curr} , the index of the current bit, is odd, $\text{ffs}^*(\text{bin}(i_{curr})) = 0$, and $i_{dest} = i_{curr} - 1$, we can calculate the decision LLR, $\lambda_0^{i_{dest}}$, directly according to f -node operation without any need to update the intermediate LLRs. As a consequence, when moving back to bit index $i_{dest} < i_{curr} - 1$, we need to consider the ffs^* of $i_{curr} - 1$ and/or $i_{dest} - 1$ if i_{curr} and i_{dest} both or either one is odd. This is controlled in lines 1-4 of Algorithm 3. Note that the stages to be updated are not necessarily $s = \text{ffs}^*(\text{bin}(i_{dest})), \dots, 1, 0$, but the deepest stage to be updated, s_{max} , is

$$s_{max} = \{\max(s) : s = \text{ffs}^*(\text{bin}(i_m)), i_{dest} \leq i_m \leq i_{curr}\} \quad (8)$$

The relation (8) finds the deepest stage in the factor graph at which the LLRs have been updated/overwritten during decoding from bit i_{dest} to i_{curr} . If $s_{max} > \text{ffs}^*(\text{bin}(i_{dest}))$, we need to move back further to the bit i_{-1} at which $s_{max} = \text{ffs}^*(\text{bin}(i_{-1}))$ in order to update the intermediate LLRs of the stage(s) that have been overwritten. The subroutine *findsMaxPos* in Algorithm 3 performs the operation of finding i_{-1} .

Example: Suppose the block-length is $N = 4$ and we are decoding bit $i_{curr} = 3$. The intermediate LLRs vector is $[\lambda_1^3, \lambda_1^2]$, excluding the decision LLR, λ_0^3 (see Fig. 2). Now, if we need to go one step back to bit $i_{dest} = 2$, since $i_{curr} = 3$ is odd, we do not need to update the intermediate LLR vector, i.e., λ_0^2 can be directly calculated. However, for moving back to $i_{dest} = 1$, since i_{dest} is odd, we need to find $s_{max} = 1$ and calculate $[\lambda_1^1, \lambda_1^0]$. Then it is possible to calculate the decision LLR λ_0^1 .

Note that the partial sums vector, β , is also updated in lines 9 and 12 during the aforementioned process.

Algorithm 3 shows an efficient approach for updating the intermediate LLRs. Note that the two subroutines *updateLLRs(.)* and *updatePartialSums(.)* in this algorithm and the rest of the paper are implemented similar to conventional SC and SCL decoding algorithms. This algorithm is a subroutine of Algorithm 6 which handles the backtracking for the core algorithm of Fano decoding shown in Algorithm 4. Note that the Fano algorithm proposed here stores the path metric of good and bad branches as well as memory states along the current path. Also, there is a vector named δ_j that indicates whether a good branch ($\delta_j = 0$) or bad branch ($\delta_j = 1$) is chosen to follow at bit j .

A. Heuristic Path Metric

The Fano path metric for each examined node plays an important role in the backtracking since it provides an indication for how likely it is that the partial path to this node is correct. Efficient backtracking relies on this metric to a) select a point to branch off the currently best (possibly erroneous) path to explore promising alternative solutions and to b) abandon unlikely paths based on comparing their path metrics with the threshold T .

Algorithm 3: Updating Intermediate LLRs

input : index of destination bit i_{dest} , index of current bit i_{curr} , $\hat{\mathbf{u}}_{0,i_{curr}}$
output: the updated λ

```

1 if  $i_{curr} \% 2 \neq 0$  then
2   |  $i_{curr} \leftarrow i_{curr} - 1$ 
3 if  $i_{dest} \% 2 \neq 0$  then
4   |  $i_{dest} \leftarrow i_{dest} - 1$ 
5  $s_{dest} = \text{ffs}^*(i_{dest})$  // c.f (7)
6  $s_{max} \leftarrow s\text{Max}(i_{curr}, i_{curr})$  // c.f (8)
7 if  $s_{dest} \leq s_{max}$  then
8   |  $i_{-1} = \text{findsMaxPos}(s_{dest}, s_{max}, i_{dest})$ 
9   |  $\beta \leftarrow \text{updatePSBack}(i_{-1}, s_{max}, \hat{\mathbf{u}})$ 
10  | for  $i \leftarrow i_{-1}$  to  $i_{dest}$  do
11  |   |  $\lambda \leftarrow \text{updateLLRs}(i, \lambda, \beta)$ 
12  |   |  $\beta \leftarrow \text{updatePartialSums}(i, \hat{\mathbf{u}}_i, \beta)$ 
13 else
14 |  $\lambda \leftarrow \text{updateLLRs}(i_{dest}, \lambda, \beta)$ 
15 return  $[\lambda, \beta]$ ;
16 subroutine  $\text{updatePSBack}(i_{-1}, s_{max}, \hat{\mathbf{u}})$ :
17   |  $k \leftarrow 2^{s_{max}}$ 
18   | for  $i \leftarrow i_{-1} + 1 - k$  to  $i_{-1}$  do
19   |   |  $\beta \leftarrow \text{updatePartialSums}(i, \hat{\mathbf{u}}_i, \beta)$ 
20   | return  $\beta$ ;
21 subroutine  $\text{findsMaxPos}(s_{dest}, s_{max}, i_{-1})$ :
22   |  $s' \leftarrow s_{dest}$ 
23   | while  $s' < s_{max}$  do
24   |   |  $i_{-1} \leftarrow i_{-1} - 2$ 
25   |   | if  $i_{-1} > 0$  then
26   |   |   |  $s' \leftarrow \text{ffs}^*(i_{-1})$ 
27   |   | else
28   |   |   |  $s' \leftarrow n$ 
29   | return  $i_{-1}$ ;

```

To provide such a metric, we follow the generic approach outlined in (6): the first term corresponds to the metric in list decoding while the second term is used to account for the different candidate path lengths in the Fano decoding. For every partial sequence $a^{(\ell)}$, we define the following metric:

$$\mu_\ell = M(a^{(\ell)}, \mathbf{y}) = \sum_{j=0}^{n_\ell-1} \log P(\hat{u}_j^{(\ell)} | \hat{\mathbf{u}}_{0,j-1}^{(\ell)}, \mathbf{y}) + \sum_{j=n_\ell}^{N-1} \log E_{\mathbf{y}}[P(u_j | \mathbf{u}_{0,j-1}, \mathbf{y})] \quad (9)$$

The second term is an expected metric for the continuation of the partial path with length $N - n_i$. Based on our observation of the actual metric obtained during decoding with or without backtracking, a good estimation of the second term, in case of non-erroneous received signals, is $E_{\mathbf{y}}[P(u_j | \mathbf{u}_{0,j-1}, \mathbf{y})] \approx 1 - p_{e,j}$, where p_e is the error probability of the bit-channels which can be obtained from the methods used for the construction/rate-profile of polar codes.

Let us define the *expected metric* $B = E_{\mathbf{y}}[\mu_{N-1}]$ for the full-length path and the expected metric of the remaining partial path as

$$B = \sum_{j=0}^{N-1} \log(1 - p_{e,j}) \quad (10)$$

$$B_i^c = \sum_{j=i+1}^{N-1} \log(1 - p_{e,j}) = B - \sum_{j=0}^i \log(1 - p_{e,j}) \quad (11)$$

where $\log(1 - p_{e,j})$ is the *estimated branch metric*. Now, we can rewrite (9) as a recursion as follows:

$$\mu_j = \mu_{j-1} + m_j - \log(1 - p_{e,j}) \quad (12)$$

where $m_j = \log(P(\hat{u}_j | \hat{\mathbf{u}}_{0,j-1}, \mathbf{y}))$ is the actual branch metric and $\mu_{-1} = B$.

V. LOW-COMPLEXITY FANO DECODING

In this section, we introduce an adaptive path metric depending on the noise level and some different search strategies to limit the search space.

A. Adaptive Path Metric

The bit channel i with low reliability contributes to the metric update depending on the noise level, i.e., μ_i can be significantly smaller than μ_{i-1} (due to change in the magnitude and/or sign of the decision LLRs) in the presence of large channel noise. This impact on the path metric can accumulate over time leading to a significant deviation from the expected metric in (10). Recall that due to channel dependency, a change in the channel LLR of one channel can affect the other low-reliability bit channels as well. Consequently, the metric of most of the examined branches denoted by μ' in Fig. 5 are most likely greater than the threshold, i.e., $\mu'_i > T$ for $i < i_{curr}$, where i_{curr} is defined in Section IV. This causes a large delay due to the visit of many nodes during backtracking. Hence, the metric estimate for the path continuation represented by the second term in (9), is not fairly comparable with the actual metric of the current path as discussed in the previous section.

To compensate for such deviation, we suggest adapting the estimate (11) for the continuation of partial paths relative to the impact of the channel noise on the actual metric. This adaptation can be realized by a scaling factor α for the logarithm of this probability which in effect adapts the expected probability to the noise level. The effect of this scaling is as follows: $\alpha \log E_{\mathbf{y}}[P(u_j | \mathbf{u}_{0,j-1}, \mathbf{y})] = \log (E_{\mathbf{y}}[P(u_j | \mathbf{u}_{0,j-1}, \mathbf{y})])^\alpha$. Since $\alpha \geq 1$ and $P(u_j | \mathbf{u}_{0,j-1}, \mathbf{y}) < 1$, then $(E_{\mathbf{y}}[P(u_j | \mathbf{u}_{0,j-1}, \mathbf{y})])^\alpha$ becomes smaller, accounting for a larger noise variance.

The value of α is determined after visiting the nodes of the current path to some level of decoding tree. This level should cover a sufficient number of low-reliability bit-channels to reflect the noise effect on the metric fairly. Until this level/bit index denoted by i_{bu} in line 45 of Algorithm 5, we do not perform backtracking although the metric drops below the threshold, T . Then, the scaling factor is obtained by

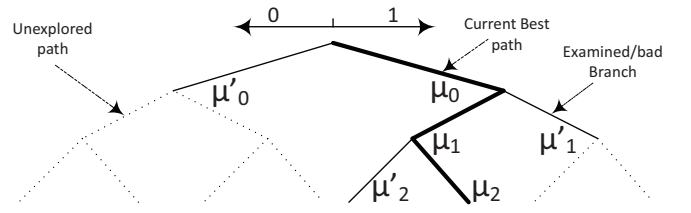


Figure 5. Decoding tree: μ_j s are the path metrics of the current best path (in bold) from the root a node at level j and the μ'_j are the path metrics of the paths diverging from the current best path.

$$\alpha = \frac{\sum_{j=0}^{n_k} \log P(\hat{u}_j^{(\ell)} | \hat{\mathbf{u}}_{0,j-1}^{(\ell)}, \mathbf{y})}{\sum_{j=0}^{n_k} \log E_{\mathbf{y}}[P(u_j | \mathbf{u}_{0,j-1}, \mathbf{y})]} \quad (13)$$

This adaptation can be performed when $\alpha > 1$, i.e., when the actual metric is larger than the expected metric. In practice, a quantized version of this factor is more convenient to use. Hence, $\alpha_q = \lceil \frac{\alpha}{\Delta_q} \rceil \Delta_q$. For instance, in decoding $PAC(128, 64)$, we first follow the current best path to bit $i_{bu} = 38$. By taking $\Delta_q = 2$ and the effect of the ceiling operator, an effective value is obtained which further reduces the complexity with almost no degradation in performance. In low and medium code rates, one can choose to calculate α after the initial sub-sequence of low-reliability bits, where the associated values in vector v are 0 (equivalent to the frozen bit-channels in polar codes).

After obtaining α , we need to update not only the metric of the current path but also the metric of the examined branches, μ'_j in Fig. 5, along the current path.

To update the computed metrics we simply add the difference between the updated bias αB_j^c and the initial bias B_j^c to μ_j and μ'_j .

$$\mu'_j = \mu'_j + (\alpha - 1) B_j^c \quad (14)$$

Thus, the metrics are computed by considering α in the next decoding steps as

$$\mu_j = \mu_{j-1} + m_j - \alpha \cdot \log(1 - p_{e,j}) \quad (15)$$

In Algorithm 4, lines 8 and 14-15 include α which is initialized in the beginning of the decoding, line 3 ($\alpha = 1$). The calculation of α and the metric updating process are shown in Algorithm 5, lines 44-51.

For hardware implementation, we are interested in simple arithmetic operations. Here, we suggest using an LLR-based metric instead of the metric based on the probability. To this end, we need to define m_j based on λ_0^j .

$$\begin{aligned} m_j(\lambda_0^j, \hat{u}_j) &= \log(P(\hat{u}_j | \hat{\mathbf{u}}_{0,j-1}, \mathbf{y})) = \log\left(\frac{e^{(1-\hat{u}_j)\lambda_0^j}}{e^{\lambda_0^j} + 1}\right) \\ &= \log\left(1 + e^{-(1-2\hat{u}_j)\lambda_0^j}\right)^{-1} \end{aligned} \quad (16)$$

where the last equality holds only for $\hat{u}_j = 0$ and 1. Now, if $\hat{u}_j = \frac{1}{2}(1 - \text{sgn}(\lambda_0^j))$, the term $e^{-(1-2\hat{u}_j)\lambda_0^j} = e^{-|\lambda_0^j|}$ is small and hence $\log(1 + e^{-|\lambda_0^j|}) \approx 0$. Otherwise, we can approximate $\log(1 + e^{|\lambda_0^j|}) \approx |\lambda_0^j|$. The term $\log(1 - p_{e,j})$

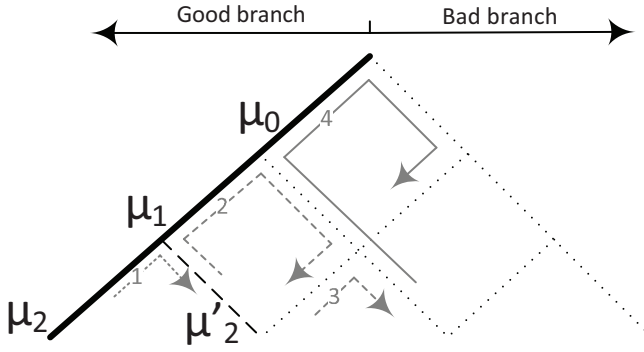


Figure 6. Bottom-up backtracking

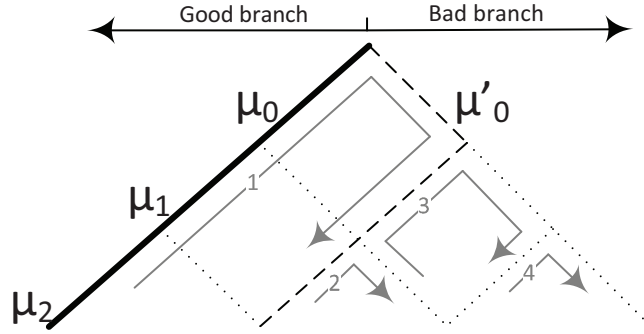


Figure 7. Top-down backtracking

and $B = \sum_{j=0}^{N-1} \log(1 - p_{e,j})$ can be computed offline and can be used in the metric computation.

Note that all the terms in (15) are negative and so are the metric values. To save one bit per metric in the storage, we can discard the bit representing the negative sign from the values. In this case we should modify the comparisons in the algorithms accordingly.

B. Constrained Tree Search

The tree search algorithm may explore the paths on the tree that are unlikely to be correct. Unfortunately, the threshold T can only be used to prune a subset of these paths since a too tight threshold would also be likely to prune the correct path. Prior knowledge about error occurrence can be used in order to constrain the tree traversal. In the following, we propose several effective constraints that result in a significant reduction in time complexity at a small performance degradation:

1) Constraint on Number of Diversions from Best Path

By using a genie that corrects the error occurrence due to channel noise, we can observe that less than 1% of the frame errors are due to more than $b = 5$ (independent) bit-errors caused by the channel noise. Fig. 8 shows the relative frequency of error occurrence for different numbers of bit-errors.

With this knowledge, we can avoid exploring the paths that diverge from the SC path at more than 5 bit-positions. If we can afford a degradation of error correction performance, we can reduce the maximum number of diversions during exploring the alternative paths. This would limit the number of visited nodes. For the example shown in Fig. 8, this number

Algorithm 4: PAC Fano Decoding

input : the channel output $\lambda_{\mathbf{r}}^{0,N-1}$, \mathcal{B} , \mathbf{g} , Δ
output: the information bits $\hat{\mathbf{d}}$

```

1  $CS \leftarrow \text{generateCS}(\mathcal{B})$  // Critical set [13]
2  $cState[1,\dots,|g|-1] = [0,\dots,0]$  // Current state
3  $[i, j, \beta, toDiverge, b_{-1}, \alpha_q] \leftarrow [0, 0, \{0\}, False, B, 1]$ 
4 while  $i < N$  do
5    $\lambda_0^i \leftarrow \text{updateLLRs}(i, \lambda, \beta)$ 
6   if  $i \notin \mathcal{B}$  then
7      $[\hat{u}_i, cState] \leftarrow \text{conv1bitEnc}(0, cState, \mathbf{g})$ 
8      $\mu_i \leftarrow \mu_{i-1} + m(\lambda_0^i, \hat{u}_i) - \alpha_q \cdot \log(1 - p_{e,j})$ 
9      $\beta \leftarrow \text{updatePartialSums}(i, \hat{u}_i, \beta)$ 
10     $i \leftarrow i + 1$ 
11  else
12     $[\hat{u}^{(0)}, cState^{(0)}] \leftarrow \text{conv1bitEnc}(0, cState, \mathbf{g})$ 
13     $[\hat{u}^{(1)}, cState^{(1)}] \leftarrow \text{conv1bitEnc}(1, cState, \mathbf{g})$ 
14     $\mu^{(0)} \leftarrow \mu_{i-1} + m(\lambda_0^i, \hat{u}^{(0)}) - \alpha_q \cdot \log(1 - p_{e,j})$ 
15     $\mu^{(1)} \leftarrow \mu_{i-1} + m(\lambda_0^i, \hat{u}^{(1)}) - \alpha_q \cdot \log(1 - p_{e,j})$ 
16     $[\mu_{max}, \hat{v}_{max}, \mu_{min}, \hat{v}_{min}] = \text{maxMin}(\mu^{(0)}, \mu^{(1)})$ 
17    if  $\text{onMAINpath} = True$  and  $\text{isBackTracking} = True$  then
18      if  $\mu_{min} > T$  and  $CS[j] = 1$  and  $j_{end} > j$  then
19         $[\text{onMAINpath}, \delta_j^s, j_{stem}] \leftarrow [False, 1, j]$ 
20         $[\lambda^s, \beta^s] \leftarrow [\lambda, \beta]$ 
21      else if  $j_{end} = j$  then
22         $\text{isBackTracking} = False$ 
23         $T = \lfloor \frac{\mu_{max}}{\Delta} \rfloor \Delta$ 
24      if  $\mu_{max} > T$  then
25        if  $\text{toDiverge} = False$  then
26           $[\hat{v}_i, \hat{u}_i] \leftarrow [\hat{v}_{max}, \hat{u}^{(\hat{v}_{max})}]$ 
27          if  $\text{onMAINpath} = True$  and  $\delta_j^s = 1$  then
28             $[\mu_i, \mu'_i] \leftarrow [\mu_{max}, \mu_{min}]$ 
29          else
30             $[\mu_i, \mu'_i] \leftarrow [\mu_{max}, \mu'_i]$ 
31           $\delta_j \leftarrow 0$ 
32        else
33           $[\hat{v}_i, \hat{u}_i] \leftarrow [\hat{v}_{min}, \hat{u}^{(\hat{v}_{min})}]$ 
34           $[\mu_i, \mu'_i] \leftarrow [\mu_{min}, \mu_{max}]$ 
35           $[\delta_j, \text{toDiverge}] \leftarrow [1, False]$ 
36         $[\text{currState}[j], cState] \leftarrow [cState, cState^{(\hat{v}_i)}]$ 
37         $\beta \leftarrow \text{updatePartialSums}(i, \hat{u}_i, \beta)$ 
38         $[i, j] \leftarrow [i + 1, j + 1]$ 
39      else
40        if  $j = 0$  then
41           $T = \lfloor \frac{\mu_{max}}{\Delta} \rfloor \Delta$ 
42        else
43           $\langle \text{Go to Algorithm 5} \rangle$ 
44  return ( $\hat{\mathbf{d}} \leftarrow \text{extract}(\hat{\mathbf{v}})$ )

```

can be set to $b = 3$ or 4 bit-positions in order to reduce the number of visited node and consequently the time complexity. We will show a result after applying this constraint in Section VI. In algorithm 6, lines 21-22 implement the constraint for the maximum diversions.

2) Exploring a Subset of bad branches

The reliability of the bit-channels is known from methods such as density evolution [24]. Hence, during backtracking, we do not need to extend the partial path to the bad branches connecting to the nodes representing high-reliability bit-channels in spite of satisfying the threshold condition. Thus, we only explore the sub-paths stemmed from bad branches of the low-

Algorithm 5: Lines 43-64 in Algorithm 4

```

43 if biasUpdated = False and  $i = i_{bu}$  then
44   if  $\mu_{max} < B$  then
45      $\alpha_q = \lceil \frac{\mu_{max}}{B \cdot \Delta_q} \rceil \Delta_q$ 
46     biasUpdated = True
47     for  $k \leftarrow 0$  to  $j$  do
48        $\mu'_{\mathcal{B}[k]} = \mu'_{\mathcal{B}[k]} + (\alpha_q - 1) \cdot B_{\mathcal{B}[k]}^c$ 
49        $\mu_{\mathcal{B}[0]-1} = \mu_{\mathcal{B}[0]-1} + (\alpha_q - 1) \cdot B_{\mathcal{B}[0]-1}^c$ 
50        $\mu_{\mathcal{B}[j]-1} = \mu_{\mathcal{B}[j]-1} + (\alpha_q - 1) \cdot B_{\mathcal{B}[j]-1}^c$ 
51 currState[ $j$ ]  $\leftarrow$  cState
52 if onMAINpath = False then
53   if  $\mu''_{\mathcal{B}[j_{stem}]} < \mu_{max}$  then
54      $\mu''_{\mathcal{B}[j_{stem}]} \leftarrow \mu_{max}$ 
55 else
56    $[j_{end}, \mu_{end}] \leftarrow [j, \mu_{max}]$ 
57    $[frmMAINpath, isBackTracking] \leftarrow [True, True]$ 
58  $[T, j', toDiverge] \leftarrow moveBack(\mu'_{0,i}, j, T, \delta_{0,j}, \hat{u}, CS,$ 
   frmMAINpath) //  $\mu'_{0,i} = \mu'_0, \mu'_1, \dots, \mu'_i$ 
59 if toDiverge = False and ( $j' = j_{stem}$  or  $j' = j$ ) then
60   onMAINpath = True
61 else
62   onMAINpath = False
63  $[i, j, frmMAINpath] \leftarrow [\mathcal{B}[j'], j', False]$ 
64 cState  $\leftarrow$  currState[ $j$ ]

```

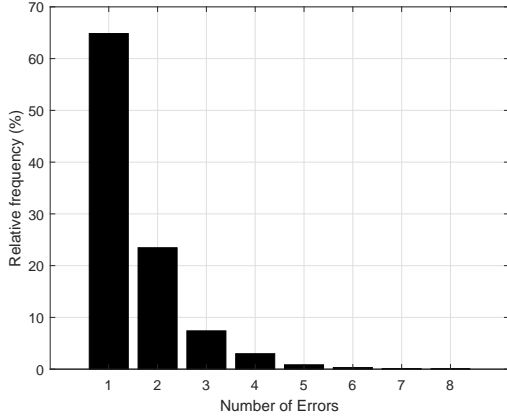


Figure 8. Distribution (in %) of the number of error occurrence, extracted from 4000 decoding failures of PAC(128,64) with RM-profile at $E_b/N_0 = 2.5$ dB

reliability bit-channels. This might introduce a small degradation (due to not exploring all the bad branches), but it reduces the time complexity significantly. To this end, we collect the indices of the low-reliability bit-channels in the critical set CS [21], [13] and in the backtracking procedure, we only compare the threshold with the metrics of bad branches exist in the critical set. Lines 6 and 20 in Algorithm 6 enforce this constraint in top-down and bottom-up schemes (discussed in the next section), respectively.

Additionally, the constraint can be set to stop decoding and declaring decoding failure when the number of steps or clock iterations exceeds some limit or the path metric drops

Algorithm 6: moveBack

```

input : the channel output  $\mu', j, T, \delta_{0,j}, \hat{u}, CS,$ 
   frmMAINpath
output:  $T, j', toDiverge,$ 
1 isMovingBack  $\leftarrow$  False
2 while True do
3    $j' \leftarrow j$ 
4   if frmMAINpath = True then // Top-down move
5     for  $k \leftarrow 0$  to  $j' - 1$  do
6       if  $\mu'_{\mathcal{B}[k]} > T$  and  $CS[k] = 1$  then
7          $[j', j_{stem}, isMovingBack] \leftarrow$ 
8            $[k, k, True]$ 
9          $[\lambda^s, \beta^s] \leftarrow [\lambda, \beta]$ 
10        break
11     if  $j' = j$  then
12       toDiverge  $\leftarrow$  False
13       return  $[T, j, toDiverge]$ 
14   else // Bottom-up move
15     for  $k \leftarrow j' - 1$  to 0 do
16       if  $j_{stem} = k$  then
17          $j' \leftarrow k$ 
18          $[\lambda, \beta] \leftarrow [\lambda^s, \beta^s]$ 
19         toDiverge  $\leftarrow$  False
20         return  $[T, j', toDiverge]$ 
21       if  $\mu'_{\mathcal{B}[k]} > T$  and  $CS[k] = 1$  then
22         if  $sum(\delta_{0,k}) \geq maxDiversions$  then
23           continue
24         if  $\delta_k = 1$  then
25            $[j', isMovingBack] \leftarrow [k, True]$ 
26           break
27   if isMovingBack = True then
28      $[i_{cur}, i_{dest}] \leftarrow [\mathcal{B}[j], \mathcal{B}[j']]$ 
29      $[\lambda, \beta] \leftarrow updateInterLLRs(i_{dest}, i_{cur}, \hat{u}_{0,i_{cur}}, \lambda,$ 
30        $\beta)$ 
31     if  $\delta_{j'} = 0$  then
32       toDiverge  $\leftarrow$  True
33       return  $[T, j', toDiverge]$ 
34     else if  $j' = 0$  then
35       toDiverge  $\leftarrow$  False
36       return  $[T, j', toDiverge]$ 

```

below a certain value. This could avoid cases with excessive runtime due to visiting a huge number of nodes. Also, we can stop decoding when the path metric drops below a certain value. Since in this case, the decoder either fails correcting the error(s) or it may lead to a long decoding delay due to visiting a huge number of nodes in order to find the correct path.

C. Direction of Backtracking Traversal

Considering the properties of PAC codes which are mainly inherited from polar codes, we can devise different strategies

that help to reduce the total number of nodes to visit during backtracking. When a decision error occurs during forward tree traversal, this error is propagated to the subsequent bits due to the sequential nature of decoding. In the conventional Fano decoding, backtracking starts from the latest decoded bit in a bottom-up direction step by step as shown in Fig. 6. For example, in a code with 3 bits, in the first backtracking iteration shown by 1 in Fig. 6, the 3rd bit diverges from the SC path, i.e., $u_0 - u_1 - \bar{u}_2$. In the 2nd backtracking iteration, the 2nd bit diverges only, i.e., $u_0 - \bar{u}_1 - u_2$. Then the 2nd and 3rd bits diverge together, i.e., $u_0 - \bar{u}_1 - \bar{u}_2$. This process continues towards the top of the tree until (in the worst case) all the combinations of 1-bit, 2-bit and 3-bit diversions are explored, assuming the threshold condition is satisfied by all the branches. However, as our observations show, the probability that the first error due to channel noise has occurred at one of the first bits is higher. On the other hand, there is no point in correcting the error that occurred due to error propagation. Thus, backtracking in a top-down fashion as shown in Fig. 7 is more consistent with the location of the first error and the subsequent propagated errors.

The top-down backtracking can only be performed on the bad branches stemmed from the SC path as a reference path. The rest of the backtracking iterations follow the bottom-up fashion. Note that a good branch is determined as a local branch with a higher likelihood among two branches stemmed from a parent node. Thus, a good branch could form a non-SC path any where on the decoding tree. However, the SC path is distinguished by following the good branches at all the decoding steps from the root to the leaf of the tree. This SC path is shown by the bold line in Fig. 6 and 7.

Choosing a bad branch in the backtracking is called a *diversion* and its corresponding metric is denoted by a prime symbol, i.e., μ' , in Fig. 6 and 7. This diversion is equivalent to flipping a bit/bits [29] from the SC path in the SC decoding. In Algorithm 6, lines 5-12 and 14-25 illustrate the implementation of the top-down and the bottom-up traversals, respectively.

D. Threshold Update Strategy

When the channel noise has a high impact on the decision LLRs of low-reliability bits, as discussed in Section V-A, the best path metric μ drops significantly over a burst of low-reliability bit-channels such that $\mu \ll T$. On the other hand, at every iteration of backtracking (i.e., exploring all the potential sub-paths stemmed from the current path), the threshold is reduced by Δ . Thus, several backtracking iterations are required to satisfy $\mu > T - m\Delta$ for $m > 1$ (m is the number of backtracking iterations). If we skip the $m - 1$ iterations and just we perform one iteration and then update the threshold at once using $T = \lfloor \frac{\mu}{\Delta} \rfloor \Delta$ to satisfy the condition $\mu > T$, we can proceed with the decoding of the current best path and avoid extra delay. There is a possibility that the correct path is not the most likely path and the decoder could find another path in one of the backtracking iterations that we are going to skip. Our observation shows that the degradation due to skipping $m - 1$ backtracking iterations is about 0.05 dB at

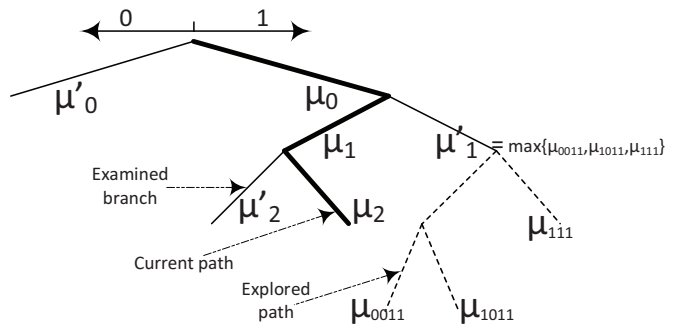


Figure 9. Updating the Metric of Explored Branches

the high SNR regime. The line 23 in Algorithm 4 shows the implementation of this strategy.

E. Updating Expected Metrics of Explored Paths

During backtracking, the sub-paths originated from the current best path through bad branches are partially explored. The exploration of the same paths (possibly with longer length) might be repeated later as we proceed with the decoding. Our aim is to benefit from the time spent to explore the sub-paths. By updating the path metric, μ'_j , at the bad branch originated from the current best path, as shown in Fig. 9, with the actual result of exploration rather than the expected path metric, we may avoid re-exploring these paths in the next cycle(s) of backtracking. Since many sub-paths might originate from the same branch, we update μ'_j with the largest metric obtained among sub-paths. This process is performed in lines 52-54 of Algorithm 5. Here, we use μ'' instead for temporarily storing the actual path metric of first sub-path explored and then comparing it with the actual metric of any new sub-path explored later. Then μ' is updated in line 31 of Algorithm 4. Note that by employing the adaptive heuristic metric, the effect of this updating becomes insignificant.

VI. NUMERICAL RESULTS

In this Section, the error correction performance and the complexity of different tree search algorithms with different setups, using the tree search reduction ideas and adaptive metric, are illustrated and analyzed. First, we describe the dispersion bound for finite block-length codes.

To obtain the numerical results in this Section, we use different rate-profiles such as Reed-Muller (RM), density evolution with Gaussian approximation, and the polarization weight (PW) [26] with minimum row-weights eliminated. Fig. 10 illustrates the aforementioned rate-profiles. Here, we briefly revise RM-profile and modified PW-profile.

1) Reed-Muller (RM) Rate-profile

The bit-channels for information bits are selected according to the row-weights ($w_i = wt(g_N^i)$ where g_N^i is the i -th row) of G_N . When the candidate bit-channels with the smallest row-weight is more than need, the more reliable ones are selected. In this case, the rate-profile is called *RM-polar* [25]. In this work, the reliability measure is the mean LLR obtained from density evolution with Gaussian approximation (DE/GA).

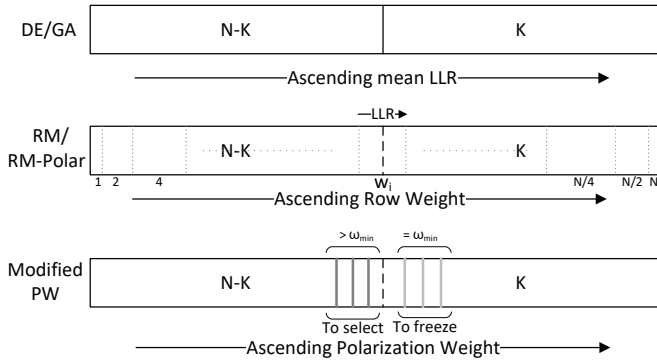


Figure 10. Rate-profile Schemes

2) A Modified Polarization Weight (PW) Rate-profile

In this method, the bit-channels for information bits are selected among the ones with the largest polarization weight (W_i), $W_i = \sum_{j=0}^{n-1} b_j \cdot 2^{j \cdot \frac{1}{4}}$, where $i = b_{n-1} \dots b_0$ is the binary representation of i [26].

In order to improve the distance property, we propose freeze the selected bit-channels with minimum row-weight and replace them with the bit-channels with lower polarization weight W_i , but larger row-weight w_i .

In the simulations, we employ different generator polynomials (0o36, 0o133, 0o177, and 0o1563 in octal format) with constraint lengths 5, 7, 7, and 10, respectively. The numerical results show that the difference among them in terms of FER is negligible in the low SNR regime and small in the high SNR regime.

Finally, for the purpose of comparison in the figures, we use the dispersion bound [8] a.k.a. Polyanskiy-Poor-Verdu (PPV) bound or finite-length bound which is a Gaussian approximation on the block error probability of finite-length block codes.

A. Distance Spectrum

As discussed in Section III, by convolutional precoding, we are no longer transmitting fixed known values, e.g., 0 frozen bits, over low-reliability (bad) synthetic channels, but random values generated by a linear combination of information bits and zero bits due to the rate-profiling. Does this difference improve the distance properties of PAC codes? To answer this question, we use the multilevel SCLD-based search method in [23] to enumerate the codewords with the minimum Hamming distance, d_{min} . We use a moderate list size of $L = 2^{15}$ and introduce in each iteration a one-bit error in the positions corresponding to the minimum row weight in P_n , when the all-zero codeword is transmitted and no noise is added. Re-encoding the candidate messages, remaining in the list at the end of decoding, shows that the number of codewords with the minimum Hamming weight $d_{min} = 16$ is $A_{16} = 1362$ for polar code $P(128, 64)$ constructed with RM-profile, whereas $A_{16} = 17$ for PAC code $PAC(128, 64)$ with the same rate profile. Furthermore, the second minimum distance for polar code is 24 with $A_{24} = 51483$ while for PAC code we observe $A_{18} = 70$, $A_{20} = 513$, $A_{22} = 2766$ and $A_{24} = 7928$. Fig. 11 compares A_d for these two codes.

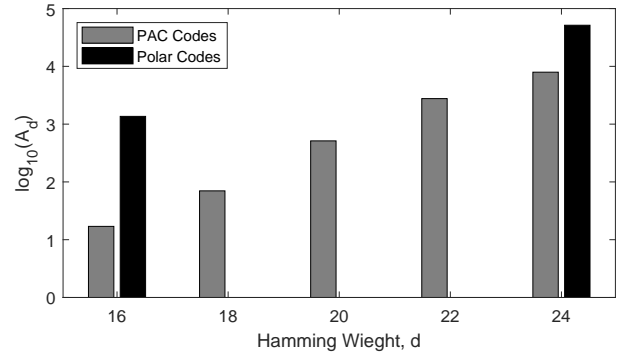


Figure 11. Partial distance spectrum of PAC(128,64) and P(128,64) with RM-profile

From the truncated union bound of the block error probability under ML decoding, $P_e^{ML} \approx A_{d_{min}} Q(2d_{min}RE_b/N_0)$ [30], we can conclude that given the same d_{min} , the code with smaller $A_{d_{min}}$ should perform better. In [31], the authors show that a properly designed upper-triangular pre-transformation matrix can reduce $A_{d_{min}}$ of the concatenated code. Note that the convolutional pre-transform G suggested for PAC codes has an upper-triangular Toeplitz matrix.

B. List Decoding

The list decoding of PAC codes over binary-input additive white Gaussian noise (BIAWGN) channel with BPSK modulation is simulated. The constraint length and the coefficients of the generator polynomial for convolutional code are 7 ($m = 6$) and 0o133, respectively. For PAC(128,64), the rate-profile is formed by the Reed-Muller (RM) construction [25] with dSNR=3.5. In the list decoding, different list sizes are employed and the performance is compared with the performance of polar code of P(128,64) and finite-length bound [8] as shown in Fig. 12. The performance of the RM-profile and the modified PW-profile are identical as the resulted rate-profiles are identical. Serial concatenation of CRC with PAC(128,64) does not improve the error correction performance. However, an 8-bit CRC with a generator polynomial with coefficients 0xA6 improves the performance of PAC(512,256) at high SNR regime significantly as shown in Fig. 12. The notation CxA-SCL used in Fig. 12 is defined as CRC-aided SCL decoding with x-bit CRC. The rate-profile for this code is formed by density evolution with Gaussian approximation (DEGA) [24] with dSNR=2. One can observe that as the block-length increases, the performance of PAC codes under list decoding cannot compete with polar codes under CRC-aided list decoding and we need to add CRC is the outer code to detect the correct path in the list decoding.

C. Fano Decoding

The Fano decoding algorithm provides a performance near the dispersion bound, but as a variable-complexity decoding scheme, its average time complexity is extremely high. The Fano decoding of PAC(128,64) with RM-profile over BIAWGN channel is simulated. Similar to list decoding, the constraint length and the coefficients of generator polynomial

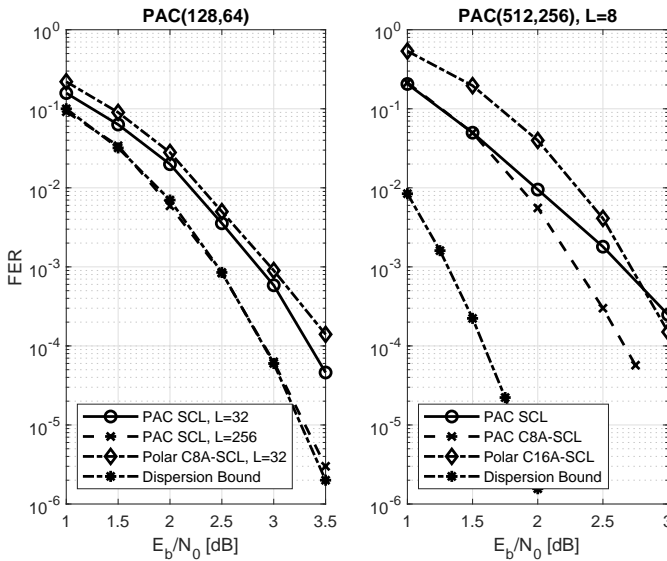


Figure 12. Performance of PAC codes under list decoding

for convolutional codes are 7 ($m = 6$) and 0o133, respectively. By applying the ideas introduced in Section IV, such as adaptive metric (AD), top-down (TD) search strategy and imposing constraint on the number of diversions (Div) from SC path it is observed in Figs. 13 and 14 that while the average time complexity drops significantly by 50% to 80%, depending on SNR and combination of techniques, the degradation in error correction performance is not high.

The time complexity is provided in terms of clock cycles. Decoding steps is not a fair metric for complexity because for every decision LLR, the number of clock cycles required for its computation varies. To compute the number of clock cycle we consider an architecture that is similar to that in [10]. In this type of design, $2N - 2$ clock cycles are required to decode a codeword [10]. However, in Fano decoding, due to possible backtracking, the number of required clock cycles might be larger than $2N - 2$. Here, we take the average clock cycles into account.

For comparison, we also implemented Fano decoding for polar codes [20]. The average computational complexities of polar codes and PAC codes under Fano decoding show a significant difference. While the poor distance spectrum of polar codes leads to a rapid candidate solution for polar codes, this solution is often incorrect and therefore the error rate performance is poor. In high SNR regime, the complexity of polar codes approaches the complexity of PAC codes when employing the aforementioned techniques.

Additionally, one can observe from the comparison of the performance of PAC(128,64) under list decoding in Fig. 12 and Fano decoding in 13 that Fano decoding provides a superior performance over list decoding with $L = 32$, while it does not require the hardware resources of list decoding and consumes less power on average, due to its reduced time complexity. Although the Fano decoder has a variable throughput and needs input and output buffers, due to its good error correction performance and low power consumption, it can be suitable for battery-powered terminals in internet of things (IoT).

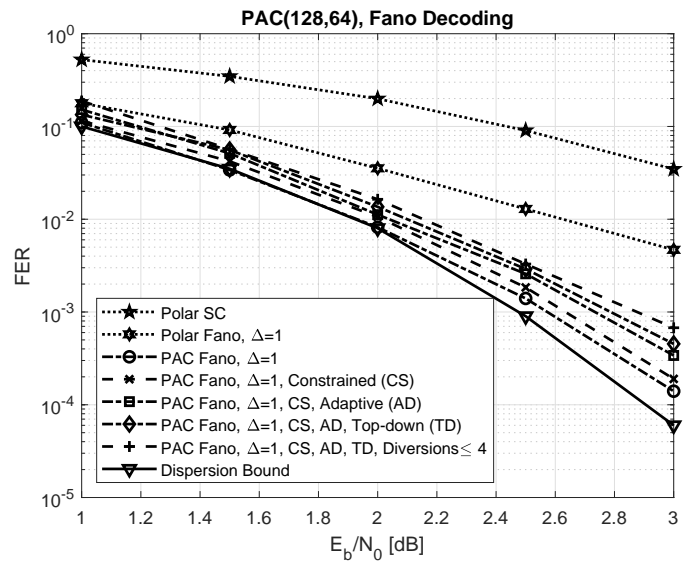


Figure 13. Performance of PAC codes under Fano decoding

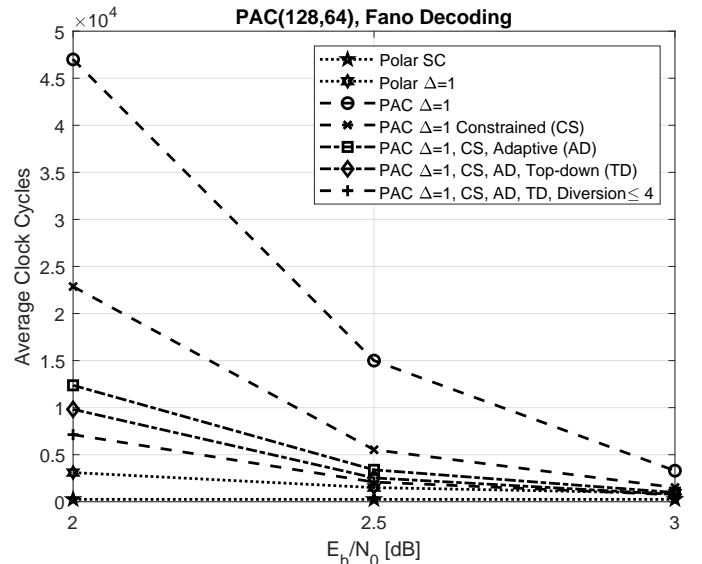


Figure 14. Average Time Complexity of Fano Decoding

VII. CONCLUSION

In this paper, we investigate the implementation of list decoding and Fano decoding for PAC codes. The results show that a large list size of $L = 256$ is needed to reach the dispersion bound. For practical list sizes, the performance gap between PAC codes and polar codes is not significant for short codes. However, the performance gap becomes large at medium block-lengths at low and medium SNR regimes. To maintain the performance gain over the high SNR regime, we need another layer of concatenation such as using CRC or parity check (PC) bits.

Fano decoding also performs close to dispersion bound at the cost of extremely large time complexity. For mitigating the large average time complexity, we propose several techniques and strategies including adaptive path metric and a heuristic to estimate a metric for the continuation of the partial paths, search constraints, and a combination of top-down and bottom-up search strategies. Also, to overcome the

difficulty of obtaining the intermediate LLRs and partial sums during backtracking, we propose an algorithm to compute these intermediate information efficiently without using extra memory to store them or any need to restart the decoding process. The numerical results show that by using these techniques, the average time complexity drops by 50% to 85% at the cost of a relatively small performance degradation. The adaptive heuristic metric and the search strategies proposed in this paper can be used in polar coding as well. Although the time complexity of the Fano Decoding is variable and high, the software Fano decoder is significantly faster than software list decoder with large list size without using parallelism.

Overall, it appears that any proper pre-transformation such as convolutional transform [7], moving parity check bits [27], dynamic frozen bits [24], use of CRC bits for error detection [6], and a combination of them can improve the distance spectrum and results in an error correction performance gain. However, each pre-transformation may provide a different gain depending on the rate-profile, block-length and code rate.

REFERENCES

- [1] E. Arıkan, "Channel polarization: A method for constructing capacity-achieving codes for symmetric binary-input memoryless channels," *IEEE Trans. Inf. Theory*, vol. 55, no. 7, pp. 3051-3073, Jul. 2009.
- [2] E. Arıkan, "On the Origin of Polar Coding," in *IEEE Journal on Selected Areas in Communications*, vol. 34, no. 2, pp. 209-223, Feb. 2016.
- [3] J. Massey, "Capacity, cutoff rate, and coding for a direct-detection optical channel," *IEEE Transactions on Communications*, vol. 29, pp. 1615-1621, Nov. 1981.
- [4] M. S. Pinsker, "On the complexity of decoding," *Problemy Peredachi Informatsii*, vol. 1, no. 1, pp. 84-86, 1965.
- [5] H. Imai and S. Hirakawa, "A new multilevel coding method using errorcorrecting codes," *IEEE Transactions on Information Theory*, vol. 23, pp. 371-377, May 1977.
- [6] I. Tal and A. Vardy, "List decoding of polar codes," *IEEE Int. Symp. on Information Theory*, St. Petersburg, Russia, Jul. 2011, pp. 1-5.
- [7] E. Arıkan, "From sequential decoding to channel polarization and back again," arXiv preprint arXiv:1908.09594 (2019).
- [8] Y. Polyanskiy, H. V. Poor and S. Verdú, "Channel Coding Rate in the Finite Blocklength Regime," *IEEE Trans. Inf. Theory*, vol. 56, no. 5, pp. 2307-2359, May 2010.
- [9] A. Balatsoukas-Stimming, M. Bastani Parizi, and A. Burg, "LLR-based successive cancellation list decoding of polar codes," *IEEE Trans. Signal Processing*, vol. 63, no. 19, pp. 5165-5179, Oct 2015.
- [10] C. Leroux, A. J. Raymond, G. Sarkis, I. Tal, A. Vardy, W. J. Gross, "Hardware implementation of successive-cancellation decoders for polar codes", *J. Signal Process. Syst.*, vol. 69, no. 3, pp. 305-315, Jul. 2012
- [11] M. Rowshan and E. Viterbo, "Stepped List Decoding for Polar Codes," 2018 *IEEE 10th International Symposium on Turbo Codes & Iterative Information Processing (ISTC)*, Hong Kong, Hong Kong, 2018, pp. 1-5.
- [12] M. Rowshan and E. Viterbo, "Improved List Decoding of Polar Codes by Shifted-pruning," 2019 *IEEE Information Theory Workshop (ITW)*, Visby, Sweden, 2019, pp. 1-5.
- [13] M. Rowshan and E. Viterbo, "Improved List Decoding of Polar Codes by Shifted-pruning," 2019 *IEEE Information Theory Workshop (ITW)*, Visby, Sweden, Aug 25-28, 2019, pp. 1-5.
- [14] M. Rowshan, E. Viterbo, R. Micheloni and A. Marelli, "Repetition-assisted Decoding of Polar Codes," in *IET Electronics Letters*, Jan 2019, DOI: 10.1049/el.2018.6940.
- [15] P. Elias, "Coding for noisy channel," in *IRE Convention Record*, vol. 3, pp. 37-46, 1955.
- [16] R. M. Fano, "A heuristic discussion of probabilistic decoding," *IEEE Trans. Inform. Theory*, vol. IT-9, pp. 64-74, 1993.
- [17] S. Lin and D. J. Costello, "Error Control Coding," 2nd Edition, Pearson Prentice Hall, Upper Saddle River, 2004, pp. 544-550.
- [18] R. Johannesson, K. S. Zigangirov, "Fundamentals of Convolutional Coding," 2nd Edition, John Wiley & Sons, Hoboken, New Jersey, 2015, pp 425-436
- [19] M. Sikora and D. J. Costello, "Supercode heuristics for tree search decoding," 2008 *IEEE Information Theory Workshop*, Porto, 2008, pp. 411-415.
- [20] M. Jeong and S. Hong, "SC-Fano Decoding of Polar Codes," in *IEEE Access*, vol. 7, pp. 81682-81690, 2019.
- [21] J. Cui, Z. Zhang, X. Zhang, H. Li and Q. Zeng, "A Low-Complexity Improved Progressive Bit-Flipping Decoding for Polar Codes," 2018 *IEEE 4th International Conference on Computer and Communications (ICCC)*, Chengdu, China, 2018, pp. 39-44.
- [22] W. Tong, "Polar Code Design Aspects and Future Challenges," *IEEE Inf. Theory Workshop*, Invited session: Polar Codes, Visby, Sweden, Aug. 2019
- [23] Q. Zhang, A. Liu, X. Pan and K. Pan, "CRC Code Design for List Decoding of Polar Codes," in *IEEE Communications Letters*, vol. 21, no. 6, pp. 1229-1232, June 2017.
- [24] P. Trifonov, "Efficient design and decoding of polar codes," *IEEE Transactions on Communications*, vol. 60, no. 11 pp. 3221-3227, Nov. 2012.
- [25] B. Li, H. Shen, and D. Tse, "A RM-polar codes," arXiv preprint arXiv:1407.5483 (2014).
- [26] X. Liu et al., " β -expansion A Theoretical Framework for Fast and Recursive Construction of Polar Codes," in *Proc IEEE Globecom*, Dec. 2017.
- [27] H. Zhang et al., "Parity-Check Polar Coding for 5G and Beyond," 2018 *IEEE International Conference on Communications (ICC)*, Kansas City, MO, 2018, pp. 1-7.
- [28] P. Trifonov and G. Trifimiuk, "A randomized construction of polar subcodes," 2017 *IEEE International Symposium on Information Theory (ISIT)*, Aachen, 2017, pp. 1863-1867.
- [29] O. Afisiadis, A. Balatsoukas-Stimming, and A. Burg, "A low-complexity improved successive cancellation decoder for polar codes," *IEEE 48th Asilomar Conference on Signals, Systems and Computers*, 2014, pp. 2116-2120.
- [30] S. Lin and D. J. Costello, "Error Control Coding," 2nd Edition, Pearson Prentice Hall, Upper Saddle River, 2004, pp. 395-400.
- [31] B. Li, H. Zhang, J. Gu, "On Pre-transformed Polar Codes," arXiv preprint arXiv:1912.06359 (2019).